The de Hass-van Alphen Effect in InBi

The de Haas-van Alphen Effect in InBi*

Yoshitami SAITO

The Research Institute for Iron, Steel and Other Metals

(Received June 5, 1964)

Synopsis

The de Haas-van Alphen effect in InBi single crystals has been studied by means of a torque method at liquid helium temperatures in magnetic fields up to 23 kilogauss. Three different oscillation periods were observed in the fields which were applied parallel to the plane including the c-axis. Each maximum period in oscillations was attained at the magnetic field parallel to the c-axis, and the periods decreased as the field was rotated. The effective masses and the collision broadening parameters were obtained from the field and temperature dependence of the amplitude of the de Haas-van Alphen oscillations. On the other hand, the de Haas-van Alphen oscillations were not observed with the fields in the case when the c-axis was set vertically. The shapes and sizes of the Fermi surfaces deduced from the three periods of oscillations above mentioned are described.

I. Introduction

The de Haas-van Alphen (dH-vA) effect is a powerful tool in investigating the electronic structure of metals, and has proved to be extremely valuable in mapping the Fermi surface of various metals. On the contrary, there have been few detailed measurements relating to the Fermi surface of compounds except for the degenerate p-type PbTe and PbS.[(1)]

In the present paper we wish to report the results of the dH-vA effect in a metallic compound, InBi[(2)].

InBi has the tetragonal PbO (BlO) type of structure, and the lattice parameters[(3)] are

$a=5.015A$, $c=4.781A$, $c/a=0.953$.

The crystal structure of InBi is shown in Fig. 1.

II. Experimental technique and samples

The instrument[(4)] used for this experiment was an automatic recording torque magnetometer similar in principle to that employed by Croft et al.[(5)] The

* The 1110th report of the Research Institute for Iron, Steel and Other Metals.

(1) P.J. Stiles, E. Burstein and D.N. Langenberg, J. Appl. Phys. Suppl., **32** (1961), 2174.
(2) Y. Saito, J. Phys. Soc. Japan, **17** (1962), 716.
(3) E.S. Makarov, Doklady Akad. Nauk S.S.S.R., **59** (1948), 899.
(4) Y. Saito, J. Phys. Soc. Japan (to be published)
(5) G.T. Croft, F.J. Donahoe and W. F. Love, Rev. Sci. Instr., **26** (1955), 360.

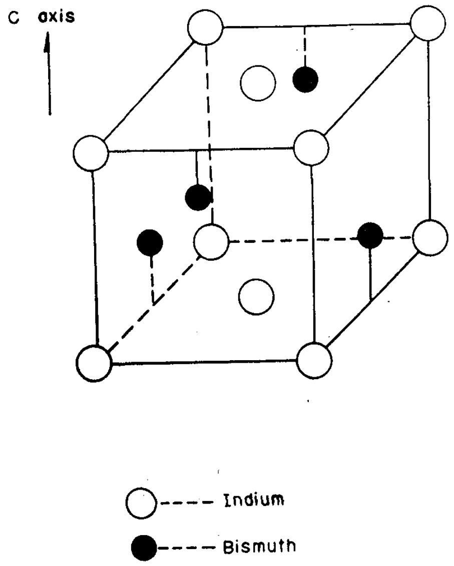

Fig. 1.

Sample Number	Sample Orientation	φ	Temperature (°K)
No. 1	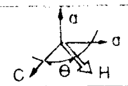	0°	1.66 2.14 4.22
No. 2	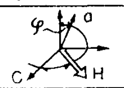	27°	1.47
No. 3	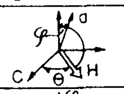	27°	1.6 ~ 1.7
No. 4	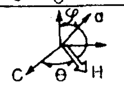	43°	1.51
No. 5	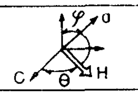	55°	1.46
No. 6	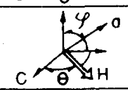	64°	1.57 4.22
No. 7	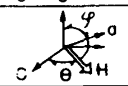	81°	1.50
No. 1′	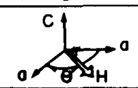		1.50

Table 1.

Fig. 1. Crystal structure of InBi.

Table 1. The relation of sample number and orientation, where θ is the angle between the vertical axis and the a-axis. Sample No. 1' is the identical with sample No. 1, but it was rotated until the c-axis vertical.

magnet system was an electromagnet with the pole faces of 10.3 cm in diameter and 65 mm gap width. In this gap, a field of 25 kilogauss was produced by flowing a current of 150A. The magnetic field strength was measured by a nuclear magnetic resonance, and the e.m.f. of a germanium Hall probe which was attached to a pole surface of the magnet was used for the field sweep of an X-Y recorder. The stability of the DC current through the magnet was better than 0.05%.

Indium of nominal purity 99.999% and bismuth of 99.9999% which were obtained from the Asahi Metal Co. Ltd. were refined by thirty zone passes at a rate of 4 cm/h in an evacuated glass tube. A mixture of bismuth and indium was sealed in an evacuated glass tube and the melt of the mixtures was kept in an electrical furnace of about 300°C for about 12 hrs. The seven single crystals of InBi were grown by the Bridgman's method.

The single crystal of InBi can be cleaved easily along the cleavage plane which is perpendicular to the c-axis of the tetragonal structure. The direction of the a-axis in the cleavage plane could easily be determined by X-ray Laue pattern.

Single crystals thus obtained were cut into about 200 mg pieces having the desired axial orientation, and samples with various orientation were attached to a quartz rod with Cemedine adhesive. The maximum misorientation of a crystal was less than 2°. The orientation of seven crystals used are illustrated in Table 1.

III. Experimental results

A typical data of the field, H, vs. torque due to the dH-vA effect in InBi sample NO. 2 is shown in Fig. 2 in the case of $\theta=20°$, where θ is the angle between H and

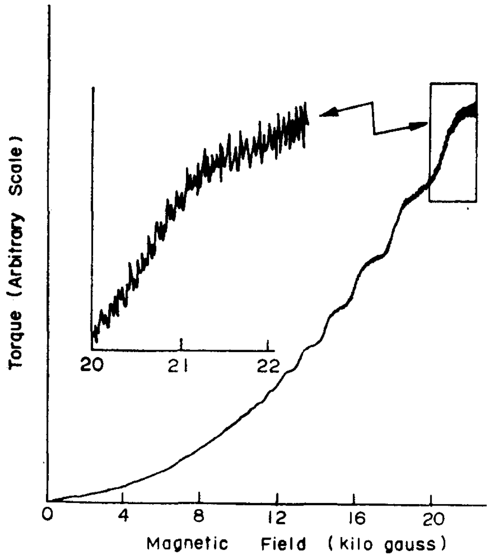

Fig. 2. A typical record of the dH-vA oscillations in the case of $\theta=20°$ at T=1.47°k, sample No. 2, where θ indicates the angle between H and the c-axis.

the c-axis. This figure shows that a longer period is revealed above 10 kilogauss, and two shorter periods — they are enlarged in this figure — are observed at higher magnetic fields. Consequently, Fig. 2 clearly displays the existence of three periods. In this paper three sets of periods are labeled as α, β, and γ oscillations in a descending order of magnitude. The medium curve of the oscillations changes with H^2 as seen from the figure. This change is ascribed to the magnetic anisotropy of InBi, and the dH-vA oscillations superimpose on this curve.

The variation of the dH-vA oscillations with H for the α oscillations is shown in Fig. 3 at various angles θ. And those in the case of the β and γ oscillations are shown in Fig. 4. All periods became hardly observable above $\theta=60°$ even at the lowest temperature and under the highest field.

The measurement in the c-axis vertical position was done with No. 1' sample, but attempts to observe the oscillations and the non-oscillatory part due to magnetic anisotropy were not successful.

IV. Analysis of experimental results

According to a modification of Landau's theory[6] by Dingle[7], the torque C

(6) L.D. Landau, Proc. Roy. Soc. (London), A**170** (1939), 341.
(7) R.B. Dingle, Proc. Roy. Soc. (London), A**211** (1952), 517.

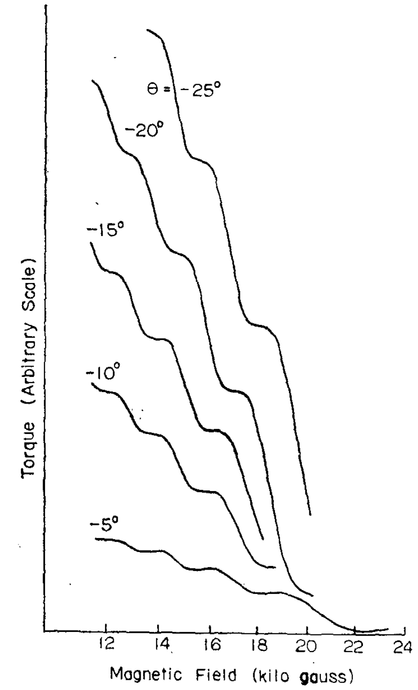

Fig. 3 (a)

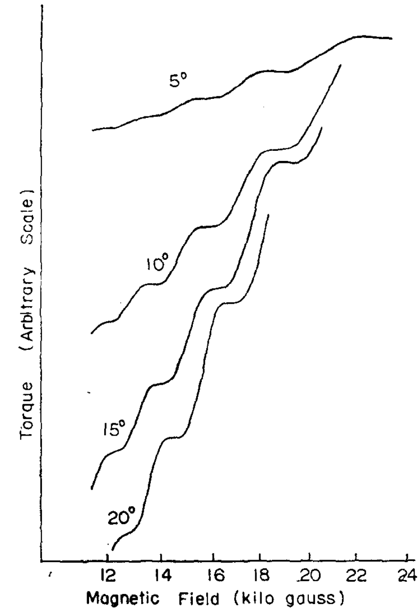

Fig. 3 (b)

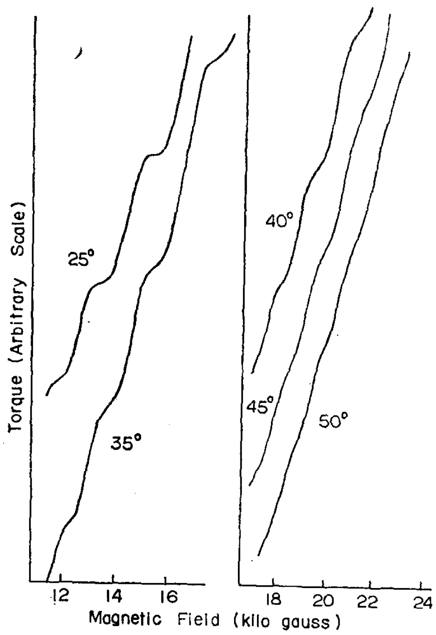

Fig. 3 (c)

Fig. 3. (a). (b). (c). The variation of the dH-vA oscillations with the magnetic field strenth for the a oscillations. (Sample No. 3)

per unit mass of the crystal is given by the following expression:

$$\frac{C}{H^2} = \sum A \frac{\Delta m}{T^{1/2}} \left(\frac{2\,\pi^2\, kT}{\beta^* H} \right)^{3/2}$$

$$\times \sum_{P=1}^{\infty} (-1)^P \frac{\exp\left(-2\pi^2 kPX/\beta^* H\right)}{2P^{1/2} \sinh\left(2\pi^2 PkT/\beta^* H\right)} \sin\left(\frac{2\pi P E_0}{\beta^* H} - \frac{\pi}{4} \right). \qquad (1)$$

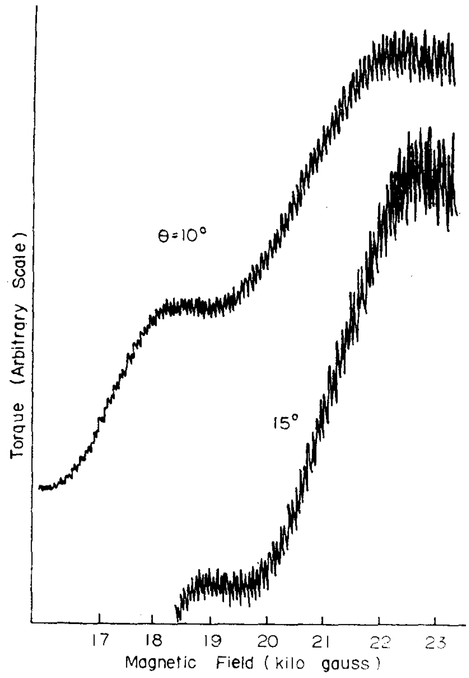

Fig. 4 (a)

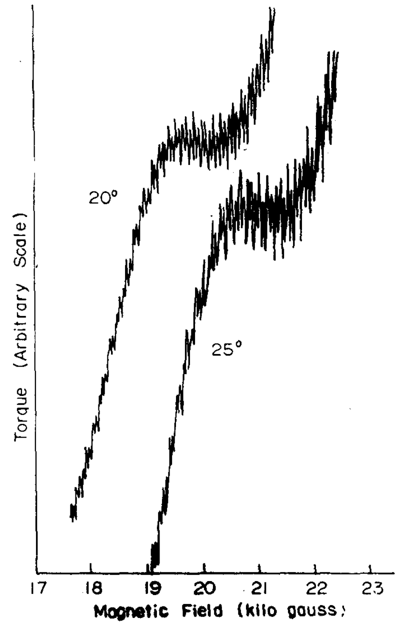

Fig. 4 (b)

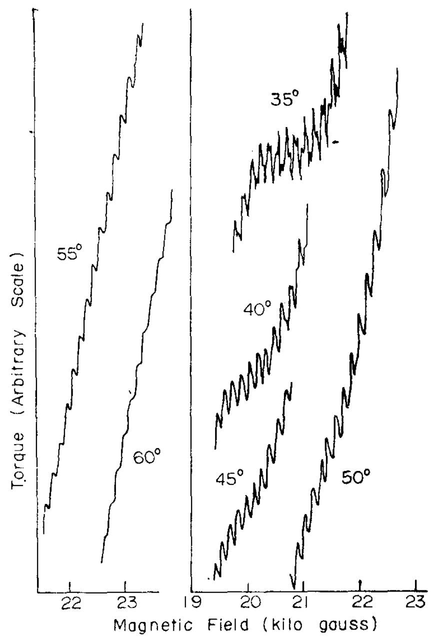

Fig. 4 (c)

Fig. 4. (a). (b). (c). The variation of the dH-vA oscillations with H for the β and γ oscillations. (Sample No. 3)

Here the sample is placed in a homogeneous magnetic field, H, in the horizontal plane. C is the vertical component of the torque resulting from such a field. A is a constant given by $A=\frac{e^2 E_0}{\pi^4 c^2 \hbar (2k)^{1/2} (m')^{2/3}}$. β^* is the double effective Bohr magneton $\beta^*=\frac{e\hbar}{m^* c}$. m*, m' and Δm are functions of the relevant effective

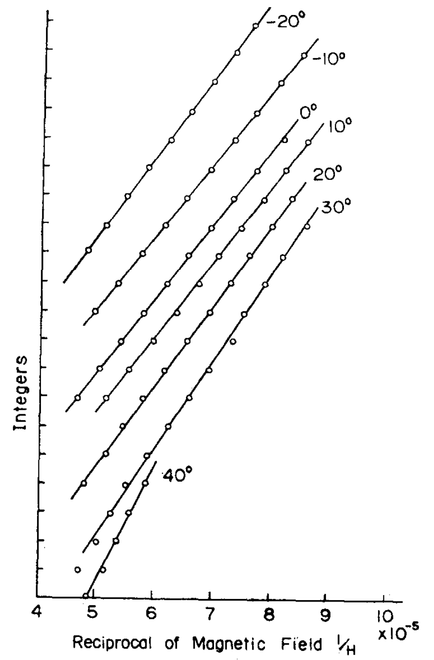

Fig. 5 (a)

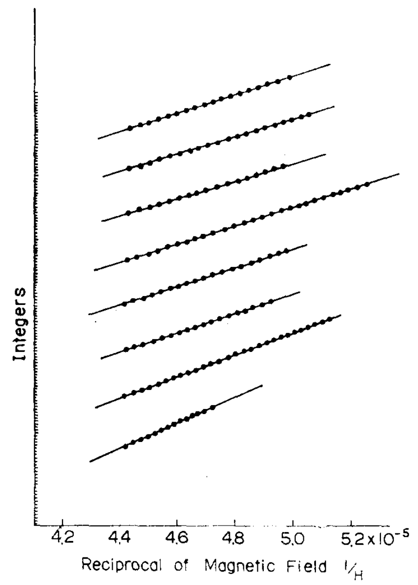

Fig. 5 (b)

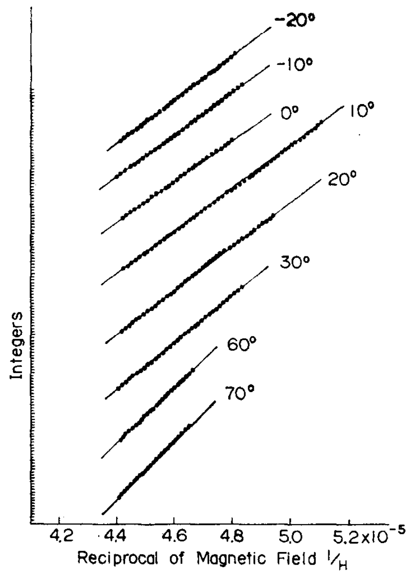

Fig. 5 (c)

Fig. 5. Plotting of the reciprocal of H corresponding to the α oscillation peaks against integers, (Sample No. 2) (a) α oscillations, (b) β oscillations, and (c) γ oscillations.

masses. E_0 is the Fermi energy, X is the Dingle factor which takes into account the level broadening due to scattering, and other symbols for physical constants have usual meanings. The first summation sign in Eq. (1) means the sum over all possible Fermi surfaces characterized by mass parameters, and the second summation is on all harmonics.

The values of the periods can be determined from the slope of the straight lines which are obtained plotting the reciprocal of H corresponding to the oscillation peaks against integers. Several examples of these results are shown in Fig. 5, corresponding to the α, β and γ oscillations.

Angular dependence of the periods obtained for three different oscillations is Fig. 6 through 8, for different samples. The maximum period is attained at $\theta=0°$

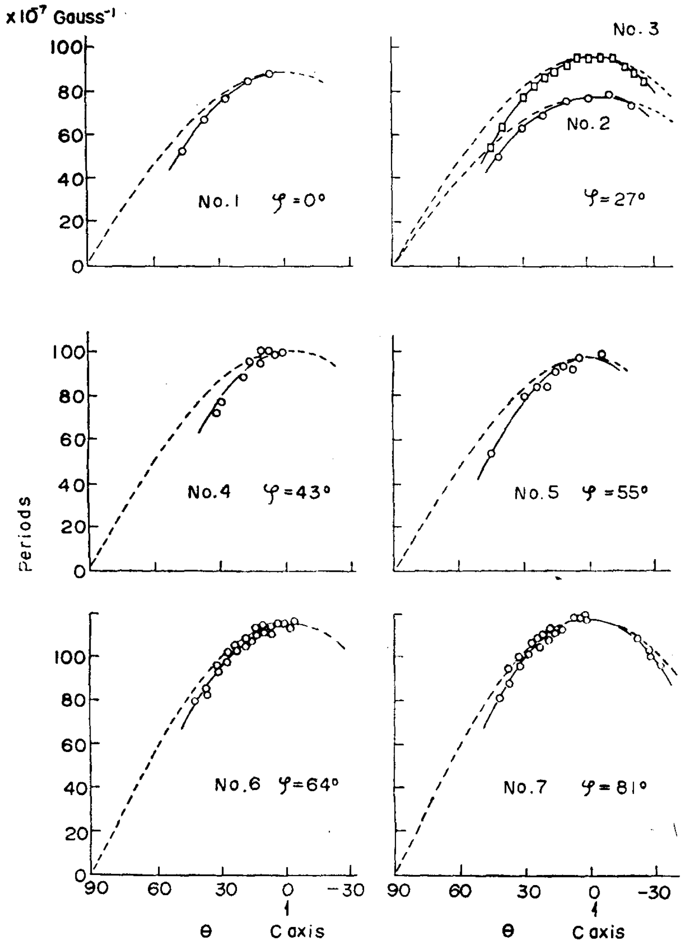

Fig. 6. Angular dependence of the periods for the α oscillations.

for all samples, and the period decreases as θ is increased. It is clear that angular dependence of the periods is symmetrical about $\theta=0°$ from these figures and the crystal symmetry of InBi. Each dashed curve in all figures is the calculated ones for an infinitely long cylinder with a maximum period fitting the experimental results at $\theta=0°$, whose axis being parallel to the c-axis.

The effective mass can be deduced from the temperature dependence of the amplitude (H and θ being kept constant). From Eq. (1), if $2\pi^2kT/\beta^*H>1$, first term of the summation is dominant comparing with the following terms. A plot of $\log\left\{\frac{a}{T}\left(1-e^{-\frac{4\pi^2kT}{\beta^*H}}\right)\right\}$ (where a is the amplitude of the oscillations)

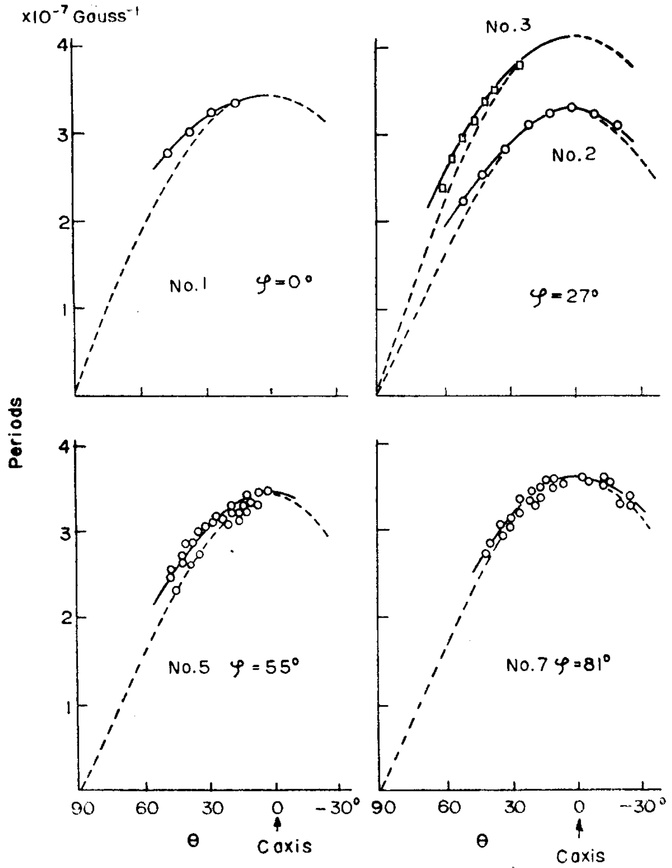

Fig. 7. Angular dependence of the periods for the β oscillations.

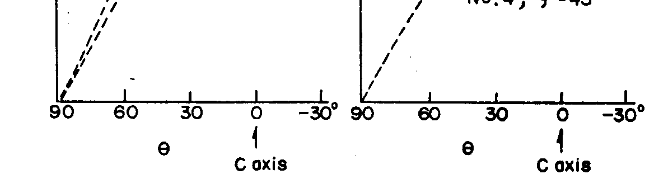

Fig. 8. Angular dependence of the periods for the γ oscillations.

against T for a fixed H should yield a straight line of slope $\frac{2\pi^2 k \log_{10} e}{\beta^* H}$ $= 6.38 \times 10^4 \frac{1}{H}\left(\frac{m^*}{m_0}\right)$. Thus, a first approximation to β^* may be obtained from the slope of the plot of log{a/T} against T. This value of β^* may then be used in log $\left\{\frac{a}{T}\left(1-e^{-\frac{4\pi^2kT}{\beta^*H}}\right)\right\}$ against T, yielding a second approximation to β^*. Then, the values of effective masses can be obtained from $\beta^*=e\hbar/m^*c$. The results of the α and β oscillations are shown in Fig. 9.

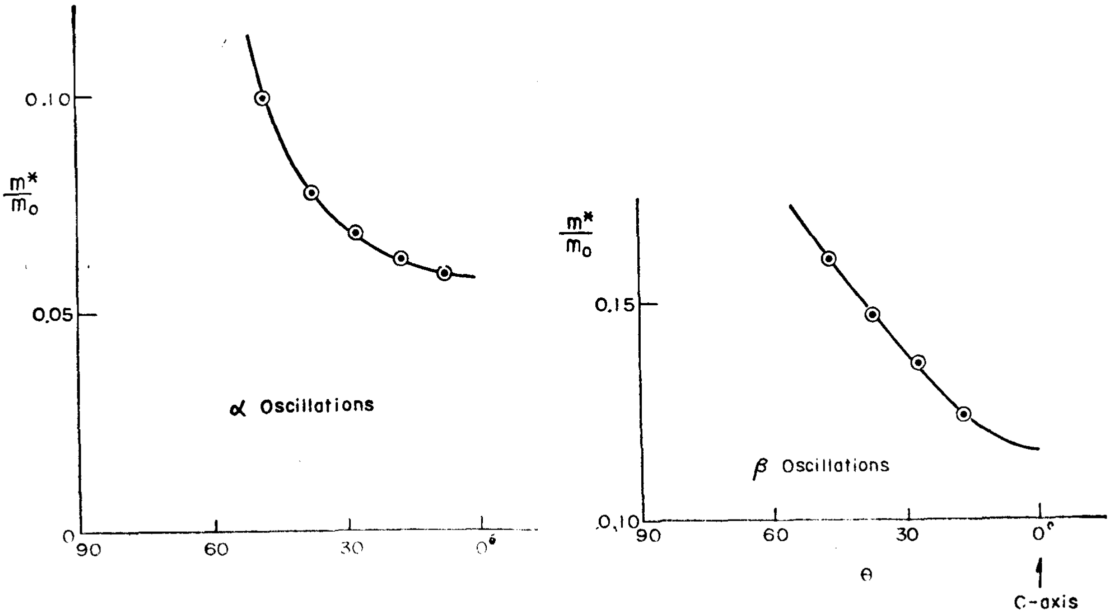

Fig. 9. Angular dependence of the effective masses.

Since the effective mass has been determined, the Fermi energy E_0 may be known from the period β^*/E_0. E_0 are estimated to be

$$E_{0\alpha} = 3.6 \times 10^{-14}\,\text{erg}\,,$$
$$E_{0\beta} = 4.1 \times 10^{-14}\,\text{erg}\,, \qquad (2)$$

corresponding to the α and β oscillations, respectively.

Dingle scattering factor X is calculated from the slope of log$\left\{aH^{3/2}\left(1-e^{-\frac{4\pi^2kT}{\beta^*H}}\right)\right\}$ against H^{-1} for a fixed T. Several such plots appear in Figs. 10 and 11 for the α and β oscillations. Thus, angular dependence of X obtained is shown in Fig. 12. Fig. 12 shows that near $\theta=30°$ X for the α oscillations is minimum. On the other hand, this figure shows that X for the β oscillations is large about $\theta=0°$, but that it decreases sharply with increasing θ.

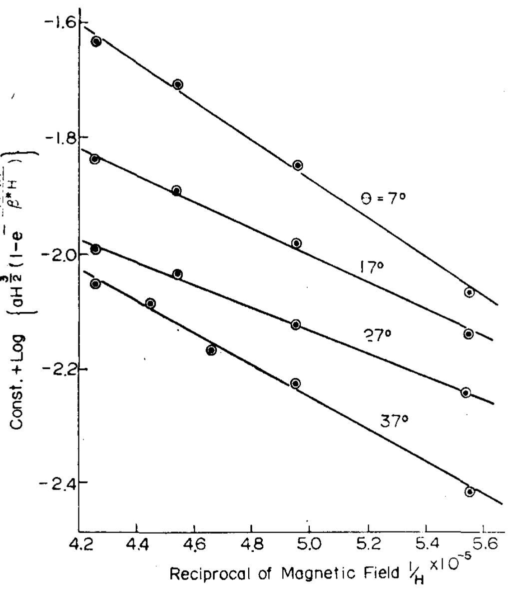

Fig. 10. Field dependence of the amplitude of the α oscillations. Values of the collision broadening parameter X are derived from the slopes of such plots.

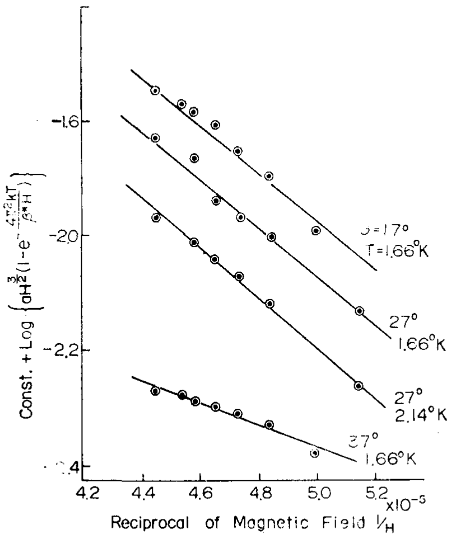

Fig. 11. Field dependence of the amplitude of the β oscillations.

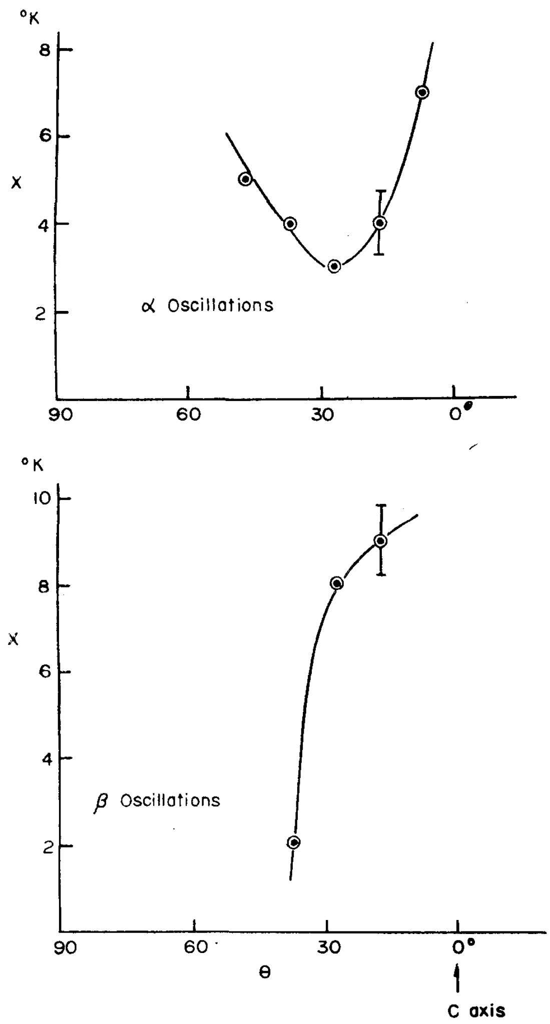

Fig. 12. Angular dependence of the collision broadening parameter X.

V. Discussion

It is interesting to explain the dH-vA effect in terms of a model of the Fermi surface. The period, P, of the oscillations is given[8] by

$$P = \frac{2\pi e}{c\hbar} \cdot \frac{1}{A_0} = 9.55 \times 10^7 \frac{1}{A_0}, \tag{3}$$

(8) L. Onsager, Phil. Mag., **43** (1952), 1006.

where A_0 is the extremal cross section of the Fermi surface cut by a plane perpendicular to H. For the Fermi surface of an infinitely long cylinder, Eq. (3) becomes

$$P = \frac{9.55 \times 10^7}{A_0} \cos\theta\ , \tag{4}$$

here θ is the angle between H and the axis of the cylinder.

It is clear from Figs. 6, 7 and 8 that each period of three different oscillations has a maximum at $\theta=0°$, and it decreases as increasing θ. Furthermore, each value of these maximum period is seen to be almost independent of θ, which is the angle between H and the a-axis. The results of this situation is shown in Fig. 13

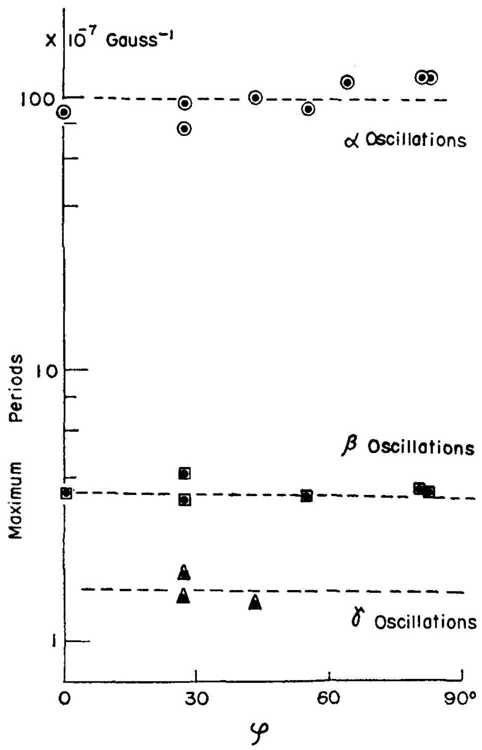

Fig. 13.

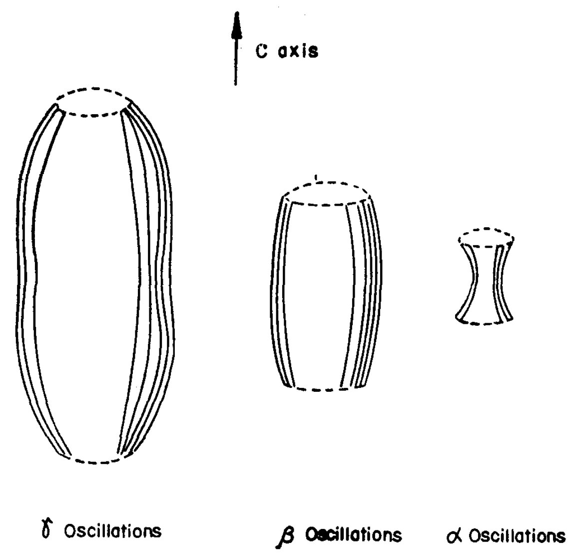

Fig. 14.

Fig. 13. φ dependence on the maximum periods at $\theta=0°$.
Fig. 14. Fermi surfaces of InBi corresponding to the α β and γ oscillations deriving from angular dependence of the periods.

(scattering of the data outside the limit of experimental error is considered to be due to the excess of indium or bismuth from the stoichiometric composition of InBi). According to this consideration, we assume that each cross section of the three infinitely long Fermi surface is circular and whose axis is parallel to the c-axis, corresponding to the α, β and γ oscillations. The dashed curves in Figs. 6, 7 and 8 are drawn according to Eq. (4), where A_0 is normalized by the experimental values at $\theta=0°$. The periods decrease approximately as the cosine of θ. But for the α oscillations the fact that the experimental points fall below the dashed curves indicates that the Fermi surface varies hyperbolically as θ is increased.

On the other hand, for β oscillations, the relation of the experimental points and solid curves varies ellipsoidally. The Fermi surfaces corresponding to each oscillation are shown in Fig. 14, and the extremal radii of the Fermi surfaces for the α, β and γ oscillations are calculated as 0.035×10^8 cm^{-1}, 0.19×10^8cm^{-1}, and 0.29×10^8cm^{-1}, respectively.

The studies of the dH-vA effect with InBi specimen, using the impulse method developed by Shoenberg, were done by Thorsen and Berlincourt(9) in 1961, and three periods of oscillation were also observed. But the orientation studied was only limited for the magnetic field within 33° from the a-axis in the plane perpendicular to the c-axis. Although we cannot directly compare our data with theirs, it seems clear by an extrapolation that the α oscillation cited above associates with their longest period, and the β and γ oscillations with the other two periods.

Acknowledgements

The author wishes to express his hearty thanks to Professor T. Fukuroi for his encouragment throughout this work. His thanks are also due to Mr. T. Fukase who prepared the crystal.

(9) A.C. Thorsen and T.G. Berlincourt, Nature, **192** (1961), 959.